

Chapter 2

PROTEOMIC ANALYSIS OF *P. AERUGINOSA* DURING
ANAEROBIC DORMANCY AND THE DISCOVERY OF SUTA,
A SLOW-GROWTH TRANSCRIPTION FACTOR.

2.1 Summary of Contributions

Published as:

- (1) Babin, B. M.; Bergkessel, M.; Sweredoski, M. J.; Moradian, A.; Hess, S.; Newman, D. K.; Tirrell, D. A. *Proc. Natl. Acad. Sci. U.S.A.* **2016**, *113*, E597–E605.

This work was performed in close collaboration with Dr. Megan Bergkessel. I performed the BONCAT proteomic screen but the efforts for the majority of the follow-up experiments were shared by me and Megan, as indicated by our co-first authorship of the associated publication. Contributions that were primarily my own include the synthesis of chemical probes, BONCAT labeling and enrichment, protein preparation and analysis of LC-MS/MS experiments, phenotypic screens of transposon mutants for biofilm formation, and immunoprecipitation and chromatin immunoprecipitation experiments. Megan's primary contributions include liquid chromatography measurements of phenazine concentrations, microscopy and analysis of the survival competition experiment, GFP fluorescence measurements, quantitative PCR measurements of transcript abundances, next generation sequencing and data analysis for RNA-Seq and ChIP-Seq experiments. We shared the following work equally: generation of plasmids and mutant strains, experimental planning, data interpretation, and writing of the manuscript.

2.2 Abstract

Microbial quiescence and slow growth are ubiquitous physiological states, but their study is complicated by low levels of metabolic activity. To address this issue, we used a time-selective proteome labeling method (bio-orthogonal non-canonical amino acid tagging; BONCAT) to identify proteins synthesized preferentially, but at extremely low rates, under anaerobic survival conditions by the opportunistic pathogen *Pseudomonas aeruginosa*. One of these proteins is a transcriptional regulator that has no homology to any characterized protein domains, and is post-transcriptionally upregulated during survival and slow growth. This small, acidic protein associates with RNA polymerase and chromatin immunoprecipitation (ChIP) followed by high-throughput sequencing suggests that it associates with genomic DNA through this interaction. ChIP signal is found both in promoter regions and throughout the coding sequences of many genes, and is particularly enriched at ribosomal protein genes and in the promoter regions of ribosomal RNA genes. Deletion of the gene encoding this protein affects expression of these and many other genes, and impacts biofilm formation, secondary metabolite production, and fitness in fluctuating conditions. On the basis of these observations, we have designated the protein SutA (survival under transitions).

2.3 Introduction

Pseudomonas aeruginosa is a cosmopolitan bacterium, notorious as a dominant opportunistic pathogen of burn wounds, medical devices, and the lungs of cystic fibrosis (CF) patients. Its genome is large and encodes an unusually high proportion of regulators [1]. Compared to *Escherichia coli*, *P. aeruginosa* possesses more σ factors that direct RNA polymerase (RNAP) to promoter regions (24 vs. 7), more DNA-binding activators and repressors that enhance or prevent RNAP binding and transcription (550 vs. 150) [2, 3], and more small, noncoding RNAs (ncRNAs) that modulate the stability or translation of target transcripts (200 vs. 100) [4, 5]. Much effort has been directed toward understanding the mechanisms by which this regulatory capacity governs the behaviors—such as quorum sensing, protein secretion, secondary metabolite production, and biofilm formation—that contribute to *P. aeruginosa* virulence.

The physiological states of bacteria involved in chronic infections are substantially different from those most often studied in standard laboratory experiments; chronic infections are characterized by slow growth rates imposed by limited nutrients or oxidants, or by host immune responses. Direct measurements of *in situ* microbial growth rates in the context of lung infections in CF patients have revealed doubling times of several days [6]. Measurements of expectorated sputum show that hypoxic and anoxic zones exist within infected CF airways, and can experience dramatic fluctuations in redox potential [7]; *P. aeruginosa* strains isolated from the CF lung show gene expression patterns consistent with adaptations to hypoxia [8], suggesting that a lack of oxygen may limit growth. While *P. aeruginosa* can generate energy in this environment by using nitrate as the terminal electron acceptor for respiration [9], levels of nitrate may be too low or too variable for this to represent the sole energy source in anoxic zones. *P. aeruginosa* can also remain viable for weeks in an anaerobic survival state by carrying out substrate-level phosphorylation to generate ATP, using either pyruvate (assisted by phenazines [10] or arginine as a carbon and energy source [11, 12]. The cells do not grow when limited to this type of metabolism, and little is known about how basic cellular processes are maintained.

We explored the *P. aeruginosa* anaerobic survival state by identifying the proteins that are synthesized in this energy-limited condition. Previous studies have characterized transcriptomic responses to low oxygen [13, 14] and have identified a few proteins that increase in abundance under conditions of anaerobic survival [15]. The potential for important post-transcriptional regulation under stress conditions [16,

17] led us to take a proteomic approach, and the low metabolic rates that occur during anaerobic survival meant that the quantity of protein made after the shift to anaerobic conditions would likely be small relative to the size of the pre-existing proteome. To address these challenges and specifically identify proteins associated with the anaerobic survival state, we used a time-selective proteome-labeling approach, referred to as bio-orthogonal noncanonical amino acid tagging (BONCAT) [18, 19] to enrich and identify proteins made during anaerobic survival. We identified 91 proteins that were preferentially synthesized under anaerobic survival conditions compared to aerobic growth conditions in the same medium. Phenotypic screens of mutants lacking these proteins led us to focus on a single uncharacterized protein that is expressed under multiple slow-growth conditions and plays a role in biofilm formation, virulence factor production, and survival under transitions between different conditions. We used a combination of co-immunoprecipitation, mass spectrometry, and sequencing to establish this protein as a novel regulator of transcription. The protein binds RNA polymerase, causes widespread changes in gene expression, and plays a direct role in the regulation of genes encoding ribosomal components.

2.4 Results

BONCAT Enables Enrichment and Identification of Proteins Synthesized at Low Rates During Anaerobic Survival

The BONCAT technique relies on pulse-labeling cultures with the methionine (Met) surrogate azidohomoalanine (Aha) (Figure 2.S1A), which is incorporated into nascent proteins by a cell's endogenous translational machinery. Aha provides a chemical handle by which newly synthesized proteins can be distinguished and physically enriched from the pre-pulse proteome (Figure 2.S1B). To probe protein synthesis during anaerobic survival on arginine, we shifted an aerobic arginine culture to anaerobic conditions, allowed cells to adapt for 24 h, and then treated them with Aha (Figure 2.1A). The total amount of incorporation of Aha into cellular protein during a 16 h pulse was approximately 4-fold lower than that observed for an aerobic sample treated for only 15 min (Figure 2.1B, Figure 2.S1C-D), providing evidence of slow, but detectable, protein synthesis during anaerobic survival. Lysates from anaerobic and aerobic cultures were treated with an alkyne-biotin affinity tag, enriched for Aha-labeled proteins with streptavidin beads (Figure 2.S1F), and analyzed by liquid chromatography-tandem mass spectrometry (LC-MS/MS).

We identified 869 proteins overall; 50 were detected only in the anaerobic sample and 273 were detected only in the aerobic sample (Figure 2.1C). For the 546 pro-

teins identified in both samples, we used label-free quantification to find proteins preferentially synthesized under each set of conditions. Peptide intensities were normalized to the total peptide intensity for each run, and the ratio for each protein was calculated as the median of its peptide ratios. We found 41 and 74 proteins whose anaerobic:aerobic ratios were significantly greater than or less than 1, respectively (Figure 2.1D). Complete proteomic results are listed in Dataset A.1. The 91 proteins that were more abundant or detected only in the anaerobic sample included proteins previously implicated in anaerobic growth or survival, such as targets of the oxygen-sensing regulator Anr: NirM, CcpR, UspK, PctA, and PA14_06000 [14, 15]. More than one third, however, are annotated as “hypothetical proteins.” We hypothesized that this list of “anaerobic hits” might contain poorly characterized proteins that play important roles in regulating slow-growth physiology. To identify general regulators, we tested the ability of transposon mutants of these genes (from a mutant library [20]) to form biofilms—another growth condition in which nutrients and oxygen are limited and cells experience low metabolic rates [21].

We looked for defects in two modes of biofilm growth: as attached biofilms on a polystyrene substrate and as colony biofilms on agar plates (Figure 2.S2A-B). Mutants for three genes showed defects in both biofilm assays: FimV, PA14_44460, and PA14_69770. FimV and PA14_44460 have previously been implicated as contributors to type II secretion—a process known to be important for biofilm formation [22]. In contrast, PA14_69770 has no homology to any characterized proteins or domains and has not been investigated to date. For this reason, we chose to study further the role of PA14_69770 in *P. aeruginosa* under survival and slow-growth conditions. Based on its contribution to fitness during transitions to and from these states, uncovered in our studies, we refer to this protein as Suta (survival under transitions).

SutA Promotes Biofilm Formation, Inhibits Pyocyanin Production, and Confers a Fitness Advantage under Fluctuating Conditions

We generated a clean deletion strain ($\Delta sutA$) and an arabinose-inducible overexpression strain ($P_{ara}:sutA$) to verify the results of the biofilm phenotype screens. Arabinose cannot support growth of *P. aeruginosa* when supplied as the sole carbon source, so does not act as a nutrient during induction of gene expression in this context. For all experiments involving arabinose-induced overexpression, arabinose was also added to the wild-type and $\Delta sutA$ strains to control for any potential physiological impacts. The deletion mutant formed smooth colony biofilms that

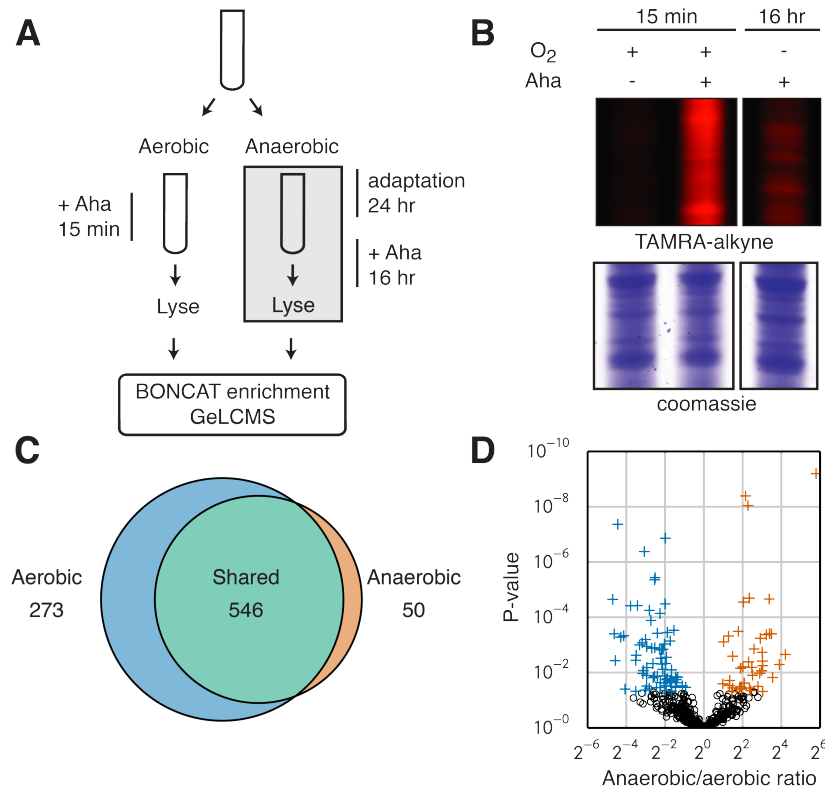


Figure 2.1: BONCAT enables enrichment and identification of proteins synthesized during anaerobic survival. (A) Overall scheme of the BONCAT experiment. (B) Lysates were treated with TAMRA-alkyne and separated via SDS-PAGE to visualize Aha incorporation. Coomassie staining indicates total protein loading (See 2.S1E for entire gel). (C) Identified proteins fell into three groups: unique to the aerobic sample, shared, and unique to the anaerobic sample. (D) Protein ratios between the two samples were calculated via label-free quantification. Proteins significantly more abundant in each sample (Benjamini-Hochberg FDR, $p < 0.05$) are marked with crosses.

lacked the complex wrinkled structures observed in wild-type biofilms, while the overexpression strain did not show substantially different colony morphology (Figure 2.2A). The deletion strain also formed smaller biofilms, and the overexpression strain larger biofilms, on polystyrene compared to the wild type (Figure 2.2B). The biofilm deficiencies of the mutant strain were not due to a growth defect, as there were no differences in growth rates between $\Delta sutA$ and the wild-type strain during aerobic planktonic culture in either rich or minimal media (Figure 2.S2C). There was, however, a strong effect of SutA on the colors of planktonic cultures; $\Delta sutA$ cultures were more blue and $P_{ara}:sutA$ cultures less blue than the wild type. This effect was pronounced under nutrient-poor conditions, following aerobic growth in

minimal medium containing pyruvate as a carbon source (Figure 2.2C). The blue color of high-density *P. aeruginosa* cultures is often due to the presence of the redox-active phenazine pyocyanin (PYO), which plays roles in signaling and virulence, and whose production is sensitive to various regulatory inputs [23–25]. We measured the concentrations of PYO and its metabolic precursor phenazine-1-carboxylic acid (PCA) in culture supernatants using HPLC and found that $\Delta sutA$ produced more PYO and less PCA than the wild type, while *P_{ara}:sutA* showed the opposite effect (Figure 2.2D). Absorbance measurements of culture supernatants gave the same results (Figure 2.S2D).

Because control of biofilm formation and phenazine production relies on integration of multiple regulatory inputs, particularly those related to changes in cell density and nutrient availability, we tested SutA's contribution to the fitness of cells exposed to changing conditions. To detect subtle effects, we competed fluorescently marked wild-type and $\Delta sutA$ strains while alternating between aerobic growth in LB and anaerobic survival in minimal arginine medium. On average, the wild-type strain significantly outcompeted $\Delta sutA$ after four transitions (Figure 2.2E), and in five out of six trials, the wild-type strain showed a clear advantage after two transitions (Figure 2.S2E), suggesting that SutA is important during transitions to and from the survival state.

SutA Upregulation During Slow Growth is Post-transcriptional

We initially focused on SutA based on its upregulation under anaerobic survival conditions, but its roles in biofilm formation and phenazine production under aerobic conditions suggested that its expression is not solely dependent on anoxia. To assay SutA expression at both the transcript and protein levels, we generated a reporter strain carrying a fusion of the *sutA* promoter, 5' untranslated region (UTR), and 3' UTR to *gfp* (*P_{sutA}:gfp*). Both 5' and 3' UTRs have previously been shown to impact transcript stability and translation [26], so our construct was designed to capture effects conferred by both regions. We measured GFP fluorescence per cell using flow cytometry during growth in LB and pyruvate minimal media, starting in mid-exponential phase (which takes longer to reach in pyruvate minimal media than in LB). In LB, reporter protein levels per cell were low during mid- and late-exponential phase (0 to 3 h) but increased up to eightfold in late stationary phase, while transcript levels (shown normalized to the level measured at time 0 in LB) varied less than twofold throughout the experiment (Figure 2.3, solid lines). In pyruvate medium, in which cells grow approximately fourfold slower compared to

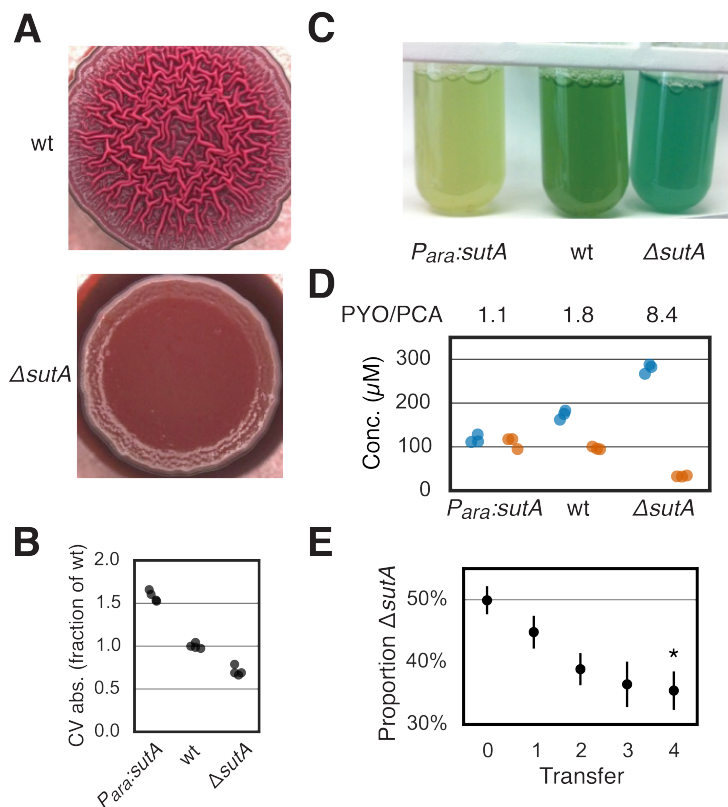


Figure 2.2: Phenotypic characterization of *sutA* mutants. (A) Colony biofilms were grown for 6 days at room temperature. (B) Biofilm growth on polystyrene was measured with the Crystal Violet assay ($n = 4$). (C) Cultures were grown in pyruvate minimal medium to stationary phase overnight at 37 °C. (D) Concentrations of PYO (blue) and PCA (orange) in culture supernatants were measured via HPLC. Average molar ratios are indicated above the plot ($n = 3$). (E) Co-cultures of wild-type and $\Delta sutA$ strains were subjected to repeated rounds of anaerobic survival followed by outgrowth to mid-exponential phase in LB. After each outgrowth, the proportion of $\Delta sutA$ was measured by fluorescence microscopy. Error bars show standard error ($n = 6$). The asterisk indicates a significant difference from the initial time point (paired Student's t-test, $p < 0.05$).

LB and remain in exponential phase for a longer time (0 to 14 h) (see also Figure 2.S2C), GFP fluorescence per cell was higher than in LB during exponential growth, and increased slightly with culture density before decreasing in late stationary phase. As in LB, normalized transcript levels showed little variation (Figure 2.3, dashed lines).

To verify that changes in fluorescence measurements reflected regulation of transcription and translation and were not due to accumulation of GFP, we constructed an analogous reporter that encoded a fusion of the promoter, 5' UTR, and 3' UTR

of the ribosomal protein gene *rpsG* to *gfp* ($P_{rpsG}:gfp$). As expected, per cell GFP expression was high in exponential phase and decreased sevenfold in stationary phase (Figure 2.S2F-H). In contrast to the *sutA* reporter construct, transcript and protein levels followed the same trend.

These results indicate that SutA upregulation occurs in conditions that cause slow growth, and does not require a lack of oxygen. Because slow growth in pyruvate minimal medium resulted in constitutive moderate expression of SutA and because we could clearly observe a phenazine phenotype resulting from SutA mutation in this medium, we chose to use late exponential phase in pyruvate minimal medium for further study of the functions of SutA.

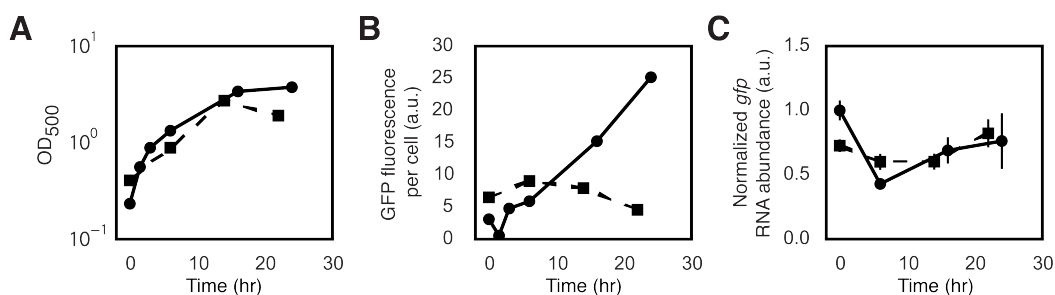


Figure 2.3: SutA upregulation during slow growth is post-transcriptional. A $P_{sutA}:gfp$ cassette was transposed into a neutral locus of the wild-type strain. (A) Optical density, (B) per-cell GFP fluorescence, and (C) *gfp* transcript abundance were measured throughout growth in LB (circles, solid lines) and pyruvate minimal medium (squares, dashed lines). Error bars represent the standard error of biological replicates ($n = 3$), and in some cases are smaller than the marker. RNA abundances were normalized by *oprI*. RNA and GFP measurements are relative to the value for the $P_{sutA}:gfp$ strain in LB at time 0.

SutA Interacts with RNA Polymerase

To gain insight into how SutA brings about the observed phenotypic changes, we sought to identify interacting protein partners. We generated an N-terminal hemagglutinin-tagged copy of SutA (HA-SutA), and verified that expression of this protein from the pMQ72 plasmid backbone in the $\Delta sutA$ background complemented the phenazine (Figure 2.4A) and biofilm (Figure 2.4B) phenotypes. We performed an immunoprecipitation (IP) against the HA epitope in this strain and in the $\Delta sutA$ strain carrying the empty pMQ72 vector following induction with arabinose in late exponential phase in pyruvate minimal medium. We identified co-precipitating proteins via LC-MS/MS analysis of the eluent fraction. Proteins co-precipitated with HA-SutA or from the empty vector control were digested with trypsin and

reacted with “medium” or “light” dimethyl labels, respectively. Peptides from both immunoprecipitations were mixed and ratios directly quantified by LC-MS/MS. In two experiments, we identified three proteins that were enriched at least fivefold in the strain expressing HA-SutA compared to the empty vector control: the α , β , and β' subunits of RNAP (RpoA, RpoB, and RpoC) (Figure 2.4C). We also detected co-precipitation of RpoA with HA-SutA in the IP eluent fraction by Western blot (Figure 2.4D). The presence of some RpoA signal in the unbound (“FT”) fraction suggests that not all cellular RNAP is tightly bound by SutA under the condition tested. We also performed the experiment in reverse by immunoprecipitating RNAP from the same cell lysates with an anti-RpoA antibody and identifying co-precipitated proteins via LC-MS/MS. When co-precipitated proteins were ordered by total peptide intensities, HA-SutA ranked above known RNAP-binders σ^{70} , NusA, and Rho (Figure 2.S3, Dataset A.2).

SutA Associates with Genomic Loci and Enhances Transcription of Ribosomal Genes

To investigate the context of the interaction between SutA and RNAP and the effects it might have on gene expression, we performed a chromatin immunoprecipitation (ChIP) -Seq experiment and an RNA-Seq experiment. The ChIP-Seq experiment was performed with the same strains and conditions used to detect the interaction with RNAP: the $\Delta sutA$ strain carrying HA-SutA on the pMQ72 arabinose-inducible plasmid and the $\Delta sutA$ strain carrying the pMQ72 empty vector as a control, both grown to late exponential phase in pyruvate minimal medium in the presence of arabinose. We cross-linked protein–DNA complexes with formaldehyde, sonicated chromosomal DNA to generate fragments 0.5 to 1 kb in length, performed immunoprecipitations against the HA epitope or against RpoA, and sequenced the co-precipitated DNA. For the RNA-Seq experiment, we sequenced rRNA-depleted RNA extracted from the wild-type, $\Delta sutA$, and $P_{ara}:sutA$ strains using the same growth medium and time point as for the ChIP-Seq experiment.

Because our IP experiment suggested that not all cellular RNAP was associated with SutA, we first sought to determine whether the interaction between SutA and RNAP occurs while RNAP is engaged in transcription, which should result in efficient formaldehyde crosslinking of SutA to genomic DNA, through concurrent interactions with RNAP. Immunoprecipitation of HA-SutA led to an average recovery of 4% of input DNA compared to 0.2% in IPs from the empty vector control strain that did not encode HA-SutA (Figure 2.S4 A), indicating that SutA likely interacts with

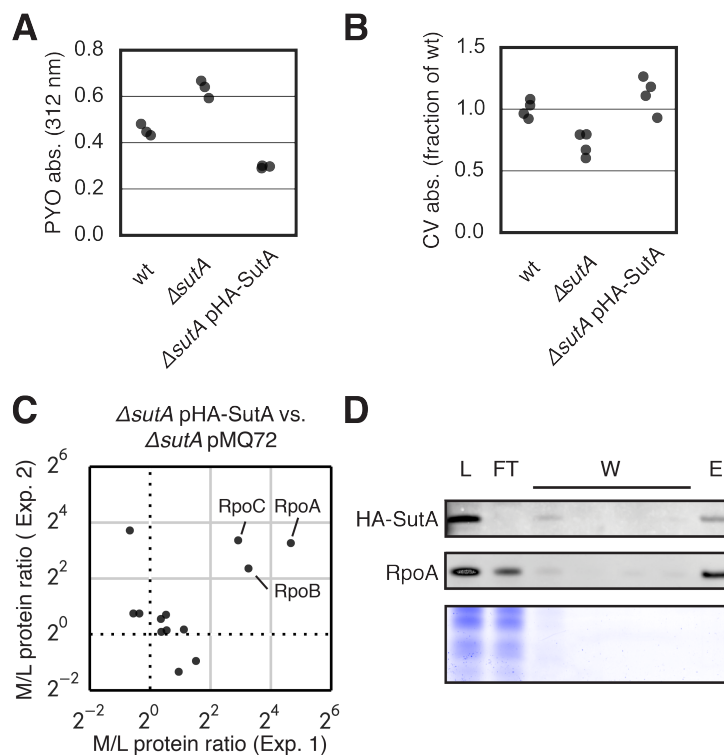


Figure 2.4: RNA polymerase co-precipitates with Suta. (A) Absorbance measurements of culture supernatants and (B) Crystal Violet (CV) measurements of biofilm formation. (C) LC-MS/MS detection and quantification of proteins co-immunoprecipitated with HA-SutA. Each axis represents the protein abundance ratio as determined by dimethyl quantification between proteins co-precipitated from the pHA-SutA (medium; M) or pMQ72 control (light; L) strains. The three main subunits of RNAP are indicated. (D) Immunoprecipitation fractions were analyzed for the presence of HA-SutA and RpoA via Western blots and for total protein via Coomassie staining (bottom). L: lysate, FT: flow-through, W: washes, E: eluent.

RNAP while RNAP is interacting with genomic DNA. Over 1,400 of the approximately 6,200 annotated genes showed a statistically significant enrichment in the HA-SutA IP compared to the empty vector IP, though the enrichment was greater than twofold for only 85 genes (Dataset A.3). We next assessed the relationship between Suta and RNAP occupancies at genomic loci by comparing average per-gene reads per kilobase per million reads mapped (rpkm) from each IP. We saw a moderately strong correlation between the associations of Suta and RpoA across all genes (Figure 2.5A, Pearson's $r = 0.77$), suggesting that Suta and RNAP tend to co-localize throughout the chromosome. This degree of correlation with RNAP ChIP signal is similar to what has been observed for NusG in *E. coli* ($r = 0.86$) and GreA in *Bacillus subtilis* ($r = 0.86$), both of which bind RNAP during transcription

elongation [27, 28]. When the ChIP data were divided into 100 bp tiles across the entire chromosome, the correlation between RNAP signal and HA-SutA signal had an r value of 0.66, which is lower than the value previously calculated in *E. coli* for DksA ($r = 0.79$) but higher than that for σ^{70} ($r = 0.57$), which dissociates from polymerase prior to transcription elongation [29]. We noted that a subset of genes had ratios of SutA ChIP signal to RpoA ChIP signal that were substantially higher than the mean for all genes, and found that many of these genes encoded ribosomal proteins (Figure 2.5A-B).

We next asked whether RNAP association at genomic loci was affected by the presence of SutA. We compared average per-gene ChIP signals for RpoA between the strain expressing HA-SutA and the strain carrying the empty vector. We found a very high correlation in per-gene RpoA ChIP signals between these two strains (Figure 2.S4B, Pearson's $r = 0.94$), suggesting that changes in the distribution of polymerase caused by the presence of SutA are subtle, or limited to a small number of loci. Although the differences in rpkm per gene were not statistically significant on an individual gene basis, we did note some departures from the overall high correlation. In particular, both ribosomal RNA (rRNA) and transfer RNA (tRNA) loci tended to show higher RpoA ChIP signals in the strain expressing HA-SutA compared to the strain lacking SutA (Figure 2.5C, Figure 2.S4D).

To establish a higher-resolution view of SutA and RNAP associations at ribosomal protein and rRNA loci, we examined ChIP-Seq reads per 100 bp tile across the relevant loci. We adapted the “apparent occupancy” metric described previously for displaying ChIP-chip data [27]. Because some non-specific immunoprecipitation of DNA is expected, the normalized read counts observed at the least expressed genes in the genome were used to define a baseline signal representing no true occupancy, and the counts observed at the highest peaks in each sample that were associated with protein coding genes were used to define a maximum signal for that sample. All count values in each sample were then scaled from 0 to 1 based on the calculated baseline and maximum values for that sample. The count values for the IP from the empty vector strain are included for comparison, and are scaled to the baseline and maximum values calculated for the HA-SutA IP to best facilitate the comparison (the dynamic range for the empty vector IP was small, as expected for a control IP in which association is non-specific) (see Supplemental Experimental Methods and Datasets A.4 and A.5 for more information).

Ribosomal protein loci exhibited distinct peaks in RNAP and SutA signal near their

transcription start sites (Figure 2.5D, Figure 2.S4C). The SutA peak was shifted very slightly downstream from the RpoA peak, and the ratio of SutA signal to RpoA signal was high over promoter and coding regions, consistent with what was observed in the per-gene analysis. The presence of SutA did not result in a significant difference in RpoA signal at any individual ribosomal protein gene locus, but across all ribosomal protein genes, there appears to be a trend toward increased RpoA signal in the presence of SutA (Figure 2.5F). Because the sequences of the four rRNA operons are nearly identical, these loci were aligned and the signals for homologous 100bp tiles from each operon were averaged (Figure 2.5E). While the rRNA genes did not show high levels of HA-SutA ChIP signal relative to RpoA ChIP signal in our per-gene analysis, this higher-resolution view shows that a very strong peak of SutA signal is centered just upstream of the start of the 16S gene, near the predicted P2 transcription start site, with a lower ratio of SutA to RpoA signal across the coding region. This view also shows a statistically significant increase in the RpoA signal at the rRNA promoter region in the presence of SutA, which was missed in our per-gene analysis. These two features are distinct from the observations for the ribosomal protein loci.

We then investigated whether the presence of SutA at ribosomal protein and rRNA genomic loci, and the changes in RNAP localization to rRNA in particular, might impact their expression. To assess the effects of SutA on ribosomal protein gene mRNA levels, we queried our RNA-Seq dataset. We measured small but statistically significant differences in mRNA abundance among the three strains for a majority of the ribosomal protein genes (46 of 55 genes, FDR-adjusted p-value < 0.05) (Dataset A.3). In general, they were expressed at higher levels in the *Para:sutA* strain, and at lower levels in the $\Delta sutA$ strain, compared to the wild-type strain (Figure 2.5F). Because the stability of mature ribosomal RNA makes it a poor indicator of rRNA transcription rates, and because rRNA was intentionally depleted from our RNA-Seq samples prior to library construction, we used qPCR against the 16S leader sequence as a proxy for levels of new rRNA synthesis. The $\Delta sutA$ strain had levels of the 16S leader that were twofold lower compared to either the wild-type strain or the overexpression strain (Figure 2.5G, Figure 2.S4E). Taken together, the ChIP and RNA abundance measurements suggest that the presence of SutA has a direct and positive effect on the transcription of both ribosomal protein and ribosomal RNA genes, but that the nature of the interactions with these two types of loci may be distinct. Extensive work by many laboratories (reviewed in [30]) has shown that regulation of rRNA transcription occurs primarily at the level of initiation while

regulation of ribosomal protein gene transcription occurs mostly during elongation. Consistent with this regulatory paradigm, our ChIP data suggest association of SutA primarily in the promoter regions of rRNA genes but throughout the coding regions of ribosomal protein genes. Also potentially consistent with these two modes of regulation, we see a decrease in RpoA ChIP signal in the absence of SutA for rRNA genes but much less so for ribosomal protein genes. Further study will be required to elucidate the mechanistic details of these two possible regulatory modes.

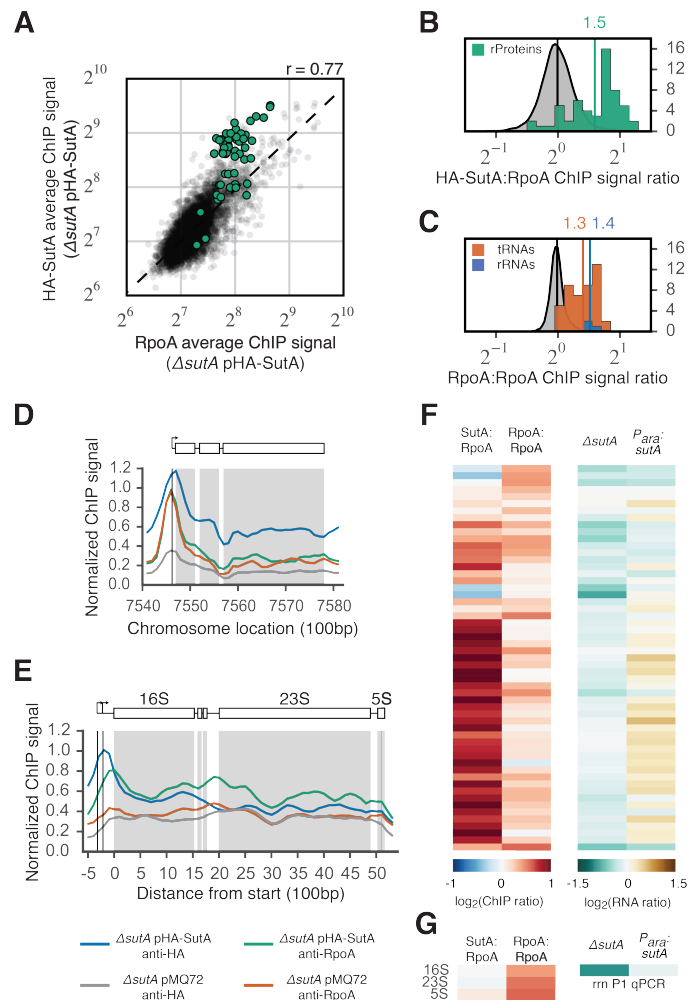


Figure 2.5: SutA localizes throughout the chromosome and enhances transcription of ribosomal genes. (A) ChIP signals (rpkm) for HA-SutA vs. RpoA for each gene. Genes encoding ribosomal proteins are highlighted (green) (Pearson's $r = 0.77$). (B) The distribution of HA-SutA:RpoA ChIP signal ratios from the $\Delta sutA$ pHA-SutA strain for all genes (gray probability density plot) and for ribosomal protein genes (green histogram). (C) The distribution of the ratios of RpoA ChIP signal from $\Delta sutA$ pHA-SutA vs. $\Delta sutA$ pMQ72 for all genes (gray probability density plot), tRNAs (orange histogram), and rRNAs (blue histogram). The mean ratios for each subset are indicated above. (D, E) Normalized ChIP signals from each IP at the *rpsLG-fusA1* ribosomal protein operon (D) and for ribosomal RNA operons (E). Legend describing strains and IPs for each trace is below. (F, G) Heat maps for ribosomal protein genes (F) and rRNA (G) showing ChIP signal ratios as calculated in (B) and (C) and transcript abundance ratios for $\Delta sutA$ and $P_{ara}::sutA$ strains, each compared to the wild-type strain as determined by RNA-Seq (F) or qPCR (G).

SutA Localizes to Many Non-ribosomal Genes and Has Broad Effects on Gene Expression

Ribosomal proteins and rRNAs are notable as classes of genes that had high levels of SutA association and whose transcript levels were significantly changed. However, the influence of SutA was not limited to these loci; much of the chromosome (approximately 20% of all 100 bp regions) showed statistically significant enrichment for the HA-SutA IP compared to the empty vector IP. To explore the general pattern of association of SutA with genomic loci, we identified a “high ChIP signal” subset of 230 transcriptional units that (i) had high-quality peaks in both RpoA and SutA ChIP signals near their starts (defined as having an apparent occupancy greater than 0.25 for RpoA and 0.20 for SutA) and (ii) showed a statistically significant enrichment in the HA-SutA ChIP signal compared to the empty vector ChIP signal. For those that had annotated transcriptional start sites and were not among the ribosomal protein and RNA genes discussed above ($n = 171$), we averaged ChIP signal values from 500 bp upstream to 1000 bp downstream of that location to generate aggregate traces of the associations of RNAP and HA-SutA across non-ribosomal loci (Figure 2.6A). The average pattern of RpoA and SutA association across these transcriptional units was similar to that observed for the ribosomal protein genes: RpoA association was centered at the transcriptional start site and a broader peak of HA-SutA was centered slightly downstream. This aggregate includes upstream regions that drive transcription of diverging transcription units as well as those for which adjacent transcription units are on the same strand, so the breadth of the observed peaks may reflect limits of the resolution of our ChIP technique as well as contributions from binding to adjacent transcriptional units.

We next investigated whether SutA association at non-ribosomal transcriptional units was also associated with increased expression. To focus on likely direct effects, we examined the 24 genes that were among the “high ChIP signal subset” and also showed greater than two-fold changes in transcript levels. 22 of these (92%) had higher transcript levels in the overexpression strain than in the deletion strain (Figure 2.6B-C), suggesting, as was observed for the ribosomal protein and rRNA genes, that the presence of SutA at these genomic loci tends to enhance their transcription. Higher-resolution views of specific loci reinforced the observations from the aggregate analysis: transcription units exhibited a broad peak of HA-SutA association centered downstream of the peak of RpoA association. PA14_10380 is predicted to encode a protein that is structurally similar to bacteriocins and is among the highest ranked-genes both in terms of SutA association and differential expres-

sion between the $\Delta sutA$ and the $P_{ara}:sutA$ strains (Figure 2.S4F) [31]. PA14_21220 encodes the universal stress protein UspK (Figure 2.S4G), and PA14_26020 encodes an aminopeptidase (Figure 2.S4H). In each of these cases, the apparent occupancy of RpoA in the promoter region is higher in the SutA-containing strain.

Many of the genes that were differentially expressed in the SutA mutants were not among the genes that showed the highest ChIP signal and many genes that had high ChIP signal did not show large SutA-dependent changes in gene expression (Figure 2.6B). This pattern is likely due to several factors. First, because the presence of SutA generally enhances transcription at loci to which it is recruited, decreased expression in the presence of SutA may be due largely to the shift of free RNAP to highly expressed loci that are upregulated by SutA (e.g., rRNA). Our data show several transcriptional units that recruit significantly more RNAP in the absence of SutA (as evidenced by higher RpoA ChIP peaks in the strain lacking HA-SutA, and no significant SutA association in the HA-SutA ChIP experiment) and that have increased expression in the $\Delta sutA$ strain; PA14_40800 and PA14_40100-40110, divergently transcribed, are two examples (Figure 2.S4I). Second, the list of genes that are likely directly regulated by SutA includes the components of the ribosome as well as known master regulators such as the stationary phase transcription factor *psrA* [32]. Increased expression of these genes is likely to cause widespread secondary effects, which may explain why some genes that are upregulated in the presence of SutA do not show strong HA-SutA ChIP signal. Third, as suggested by our analysis of rRNA and ribosomal protein genes, SutA may affect different aspects of transcription for different genes (e.g., initiation vs. elongation), with different patterns of ChIP signals and expression levels resulting. Further work is required to fully understand the impacts of SutA on different genes and different phases of gene expression.

Finally, to take a broad view of the effects of SutA, both direct and indirect, on the physiological state of the cell, we grouped the genes that differed more than twofold between the $\Delta sutA$ and the $P_{ara}:sutA$ strains according to their functional designations from the Clusters of Orthologous Groups (COG) categories [33], and asked whether any groups were differentially represented compared to the genome as a whole (Figure 2.S4J). In general, genes that were upregulated in the presence of SutA tended to have functions related to energy generation and maintenance; these genes included proteases, oxidoreductases, and alternate metabolism genes. Conversely, genes involved in growth and carbohydrate and amino acid metabolism

were significantly underrepresented. Genes that were downregulated were more likely to be involved in defense mechanisms, signaling, and motility. For the full set of results, see Dataset A.3 and GEO accession number GSE66181.

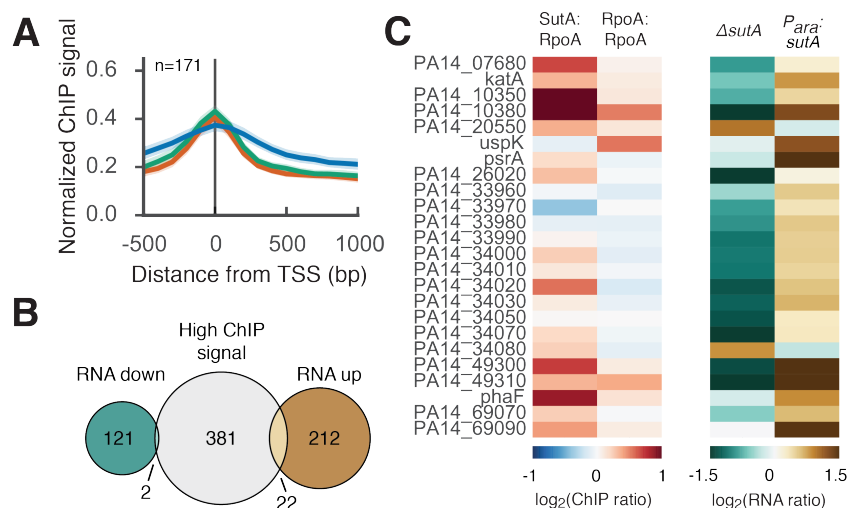


Figure 2.6: SutA has broad effects on gene expression. (A) Average ChIP signals around transcriptional start sites (TSS) for genes in the “high ChIP signal” subset. Shaded regions around each trace represent the 95% confidence interval for the mean ($n = 171$). Traces represent: $\Delta sutA$ pHA-SutA, anti-HA (blue); $\Delta sutA$ pHA-SutA, anti-RpoA (green); and $\Delta sutA$ pMQ72, anti-RpoA (orange). The direction of transcription is from left to right. (B) Numbers of genes in the “high ChIP signal” subset and genes whose expression changed more than twofold between the $\Delta sutA$ and $P_{ara}:sutA$ strains. (C) Heat maps (as in Figure 2.5F-G) for genes found in both subsets.

2.5 Discussion

While microbes have spent the majority of their evolutionary history enduring slow-growth conditions, relatively little is known about their physiology in these states. In part, this knowledge gap arises from technical challenges—slow metabolic rates and high phenotypic heterogeneity can lead to increased noise and decreased signal for many biomolecules of interest. Yet slow growth and survival states are of great relevance in many clinical and environmental contexts, and new tools are needed for their study. As illustrated here, the BONCAT method, which enables enrichment of newly synthesized proteins from large pre-existing proteomes, is well suited to the exploration of slow-growth modes of microbial life.

We used the BONCAT method to discover a previously unknown RNAP-binding factor, which we have named SutA. We found SutA to be upregulated post-transcriptionally in various growth limiting conditions. Through its interaction with RNAP, SutA lo-

calizes to many genes throughout the chromosome and elicits broad transcriptional changes. Some of these changes are likely direct effects; for example, SutA associates strongly with loci encoding ribosomal components and the transcription of these loci is reduced in the absence of SutA. Other changes may be due to secondary effects resulting from changes in the pool of free polymerase or from changes in downstream regulation by directly affected genes. Our broad analysis of transcriptional changes suggest that cells expressing SutA prioritize the expression of genes required for survival, and our phenotypic studies show that SutA is important for the establishment of biofilms, the regulation of phenazine production, and transitions to and from growth-limited states.

Understanding the molecular mechanism by which SutA effects these changes will require further study, but our observations suggest some intriguing comparisons to the well-studied regulator, DksA. DksA acts with the small molecule alarmone ppGpp during nutritional downshifts to destabilize open promoter complexes, especially at ribosomal RNA promoters. This activity reduces rRNA transcription in response to a decreased availability of nucleotides [34]. DksA can also influence elongation; it may help prevent the transition from a paused to an arrested state [35]. Interestingly, SutA appears to affect many of the same genes and phenotypes as DksA, but in the opposite direction. While DksA has been shown in both *E. coli* and *P. aeruginosa* to repress expression of ribosomal protein and rRNA genes [34, 36, 37], SutA enhances expression of these genes. Both DksA and SutA show high ChIP signal across the coding regions of highly expressed protein-coding genes, including ribosomal protein genes, and a lower signal across the coding regions of the rRNA genes. However, unlike DksA, SutA shows a high peak of ChIP signal at the promoters of rRNA genes, consistent with the observations that SutA enhances rRNA expression while DksA represses it [29]. Disruptions of DksA or SutA in *Pseudomonas* species also appear to cause opposing phenotypes: disruption of DksA causes a decrease in pyocyanin production and an increase in biofilm persistence [38, 39], while deletion of SutA causes overproduction of pyocyanin and a decrease in biofilm accumulation. Taken together, these observations suggest that a subset of genes, including the ribosomal RNA and ribosomal protein genes, are sensitive to some modulation of RNAP activity, and DksA and SutA tend to modulate this activity in opposite ways.

In our BONCAT experiment, we detected new synthesis of DksA in the aerobic exponential growth condition but not in the anaerobic survival condition. This is

consistent with a previous report that DksA is undetectable by Western blot during stationary phase in *P. aeruginosa* [36] and suggests that the repression by DksA of rRNA and ribosomal protein gene expression is downregulated during protracted slow growth. DksA is advantageous in the context of actively growing cells because it protects against “traffic jams” of stalled RNAP that obstruct the completion of DNA replication [40] and allows limited cellular resources to be directed towards expression of genes important for ameliorating the limitations (e.g., amino acid biosynthetic genes) [41]. However, for cells that are dividing infrequently or not at all, and that are limited for basic energy resources rather than specific metabolites, these functions may be counterproductive. Instead, the most adaptive response may be to maintain transcription, even at low levels, of core machinery in order to retain a capacity for cellular maintenance and to allow for a rapid upregulation of biosynthetic pathways when conditions improve. Our results suggest that SutA contributes to this type of response, and they set the stage for future biochemical and structural studies.

Recent reports have described RNAP-binding regulators that broadly affect transcription in different organisms under a range of conditions, suggesting that this is an important and diverse mode of regulation. For example, the non-essential δ subunit of *Bacillus subtilis* RNAP [39] and the recently discovered AtfA from *Acinetobacter spp.* [42] are both small proteins that, like SutA, contain highly acidic domains and broadly impact transcription, but unlike SutA, are expressed during exponential phase. CarD is a mycobacterial protein that has recently been crystallized in a complex with RNAP; unlike SutA it is essential and appears to localize primarily to promoter regions, but like SutA it broadly serves to stimulate transcription. One characteristic of all of these proteins is that they lack homologs in *E. coli*, the model organism from which much of our knowledge of bacterial transcriptional regulatory mechanisms has been derived. Each has a different phylogenetic distribution; SutA is found only in selected families of the Alteromonadales and Pseudomonadales orders of Gammaproteobacteria. This growing body of work, including the results described here, demonstrates that regulation of RNAP is diverse, and even in well-studied, clinically important pathogens, basic regulatory mechanisms governing slow growth remain to be discovered.

2.6 Experimental Procedures

For detailed descriptions of all experimental procedures, see Appendix A. Strains and plasmids used are listed in Table A.1.

Strains and growth conditions. Rich medium was Luria-Bertani (LB) broth. Minimal medium was phosphate buffered, and contained 40 mM carbon source [10]. In experiments involving *P_{ara}:sutA*, all cultures were grown in the presence of 20–25 mM arabinose. Where necessary, plasmids were maintained with the appropriate antibiotics. Aerobic growth was carried out with shaking at 37 °C. Anaerobic survival was carried out in Balch tubes in an anaerobic chamber (Coy, Grass Lake, Michigan) without shaking at 37 °C. Growth for colony morphology assays was carried out at room temperature. Genetic manipulations used standard procedures.

Biofilm measurements. Crystal Violet and colony morphology assays were carried out as previously described [43, 44].

Phenazine measurements. Phenazine concentrations in culture supernatants were determined by HPLC as previously described [25] or estimated by measuring absorbance at 312 nm.

Individual gene expression measurements. Per-cell GFP measurements were made using the Accuri c6 flow cytometer, and RNA measurements were made by qRT-PCR. Primers are listed in Table A.2.

Proteomics. BONCAT labeling, chemistry, and enrichment were performed as previously described [45]. Label-free quantitation was used for the initial screen. Relative protein abundances for immunoprecipitations were quantified via dimethyl labeling [46].

IP and ChIP. Cultures of $\Delta sutA$ pMQ72 or $\Delta sutA$ pMQ72-HA-SutA were grown to late exponential phase in pyruvate minimal medium containing 20 mM arabinose and 50 μ g/ml gentamicin. HA-SutA or RpoA was purified with anti-HA agarose beads (Thermo Scientific) or protein A/G beads (Santa Cruz Biotechnology) and an anti-RpoA antibody, respectively. Fractions were saved for Western blot analysis and eluents were analyzed via LC-MS/MS. For ChIP, cultures were grown as above, cross-linked with 1% formaldehyde, lysed via sonication, and either HA-SutA or RpoA was immunoprecipitated. Protein digestion and DNA cleanup were performed as previously described [47].

Sequencing library preparation and sequencing. For RNA-Seq, cultures of wild-type, $\Delta sutA$, and *P_{ara}:sutA* strains were grown to late exponential phase in pyruvate minimal medium containing 25 mM arabinose. Total RNA was extracted using the RNeasy Mini Kit (Qiagen) and rRNA was depleted using the Magnetic Gram Neg-

ative Bacteria RiboZero Kit (Epicentre). For ChIP-Seq, immunoprecipitated DNA was further fragmented using DS Fragmentase (NEB). Both types of libraries were prepared using the relevant Library Prep kits for Illumina (NEB). Sequencing was performed to a depth of 10–15 million reads per sample on an Illumina HiSeq2500 machine, and data analysis was performed using standard open source software, or as described in more detail in SI. Sequencing was performed on biological triplicates.

2.7 Acknowledgments

We thank Geoff Smith and Roxana Eggleston-Rangel for technical assistance with LC-MS/MS and Dr. Igor Antoshechkin for assistance with sequencing. We thank Dr. Olaf Schneewind for his gift of the anti-RpoA antibody. We appreciate constructive feedback on the manuscript from members of the Newman and Tirrell labs and Dr. Richard Gourse, as well as helpful comments from the editor and reviewers of *The Proceedings of the National Academy of Sciences*.

2.8 Supplementary Figures

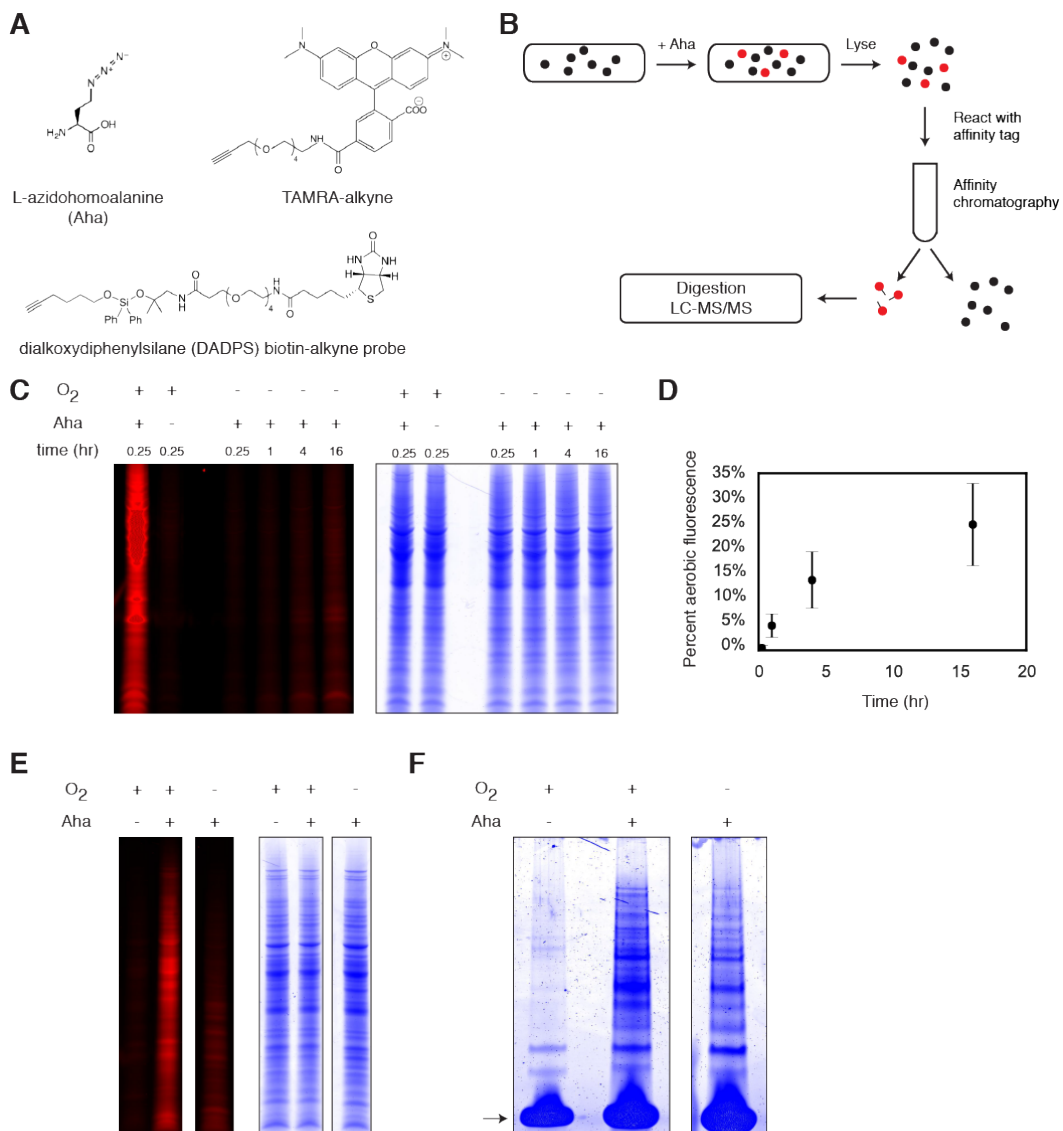


Figure 2.S1: BONCAT labeling and enrichment during anaerobic survival.

(A) Chemical compounds used for the BONCAT experiment, in-gel fluorescence detection, and protein enrichment. (B) General scheme of a BONCAT experiment. Cells are treated with Aha to initiate protein labeling. Newly synthesized proteins (red circles) are chemically distinct from pre-existing proteins (black circles) and can be reacted with an alkyne-biotin affinity tag. These proteins can be enriched via streptavidin affinity chromatography followed by cleavage of the tag, yielding a mass modification at Aha residues (black lines). Enriched proteins are digested and analyzed by LC-MS/MS. (C) Time course of Aha labeling during anaerobic survival on arginine. Cultures surviving anaerobically were treated with 1 mM Aha for the indicated time. The left two lanes show aerobically growing cultures. In-gel fluorescence of TAMRA (left) indicates Aha incorporation and Coomassie staining (right) indicates total protein loading. Images are of the same gel. (D) Quantification of relative Aha incorporation. Four regions of each lane from the gel in (C) were measured. For each lane, integrated fluorescence intensity was divided by Coomassie intensity to normalize to protein loading. Values from the anaerobic lanes were then divided by the normalized fluorescence from the aerobic culture. Error bars show the standard deviation for 4 regions from each lane. (E) The full gel lanes shown in 2.1B. Images are from the same gel. (F) Eluent fractions following BONCAT enrichment. The three samples shown in (E) were reacted with an alkyne-biotin affinity tag, bound to streptavidin beads, washed, and eluted. Eluents were concentrated and separated via SDS-PAGE. Streptavidin leached from the agarose beads is indicated with an arrow. The right two lanes were cut into eight pieces, digested, and analyzed by LC-MS/MS.

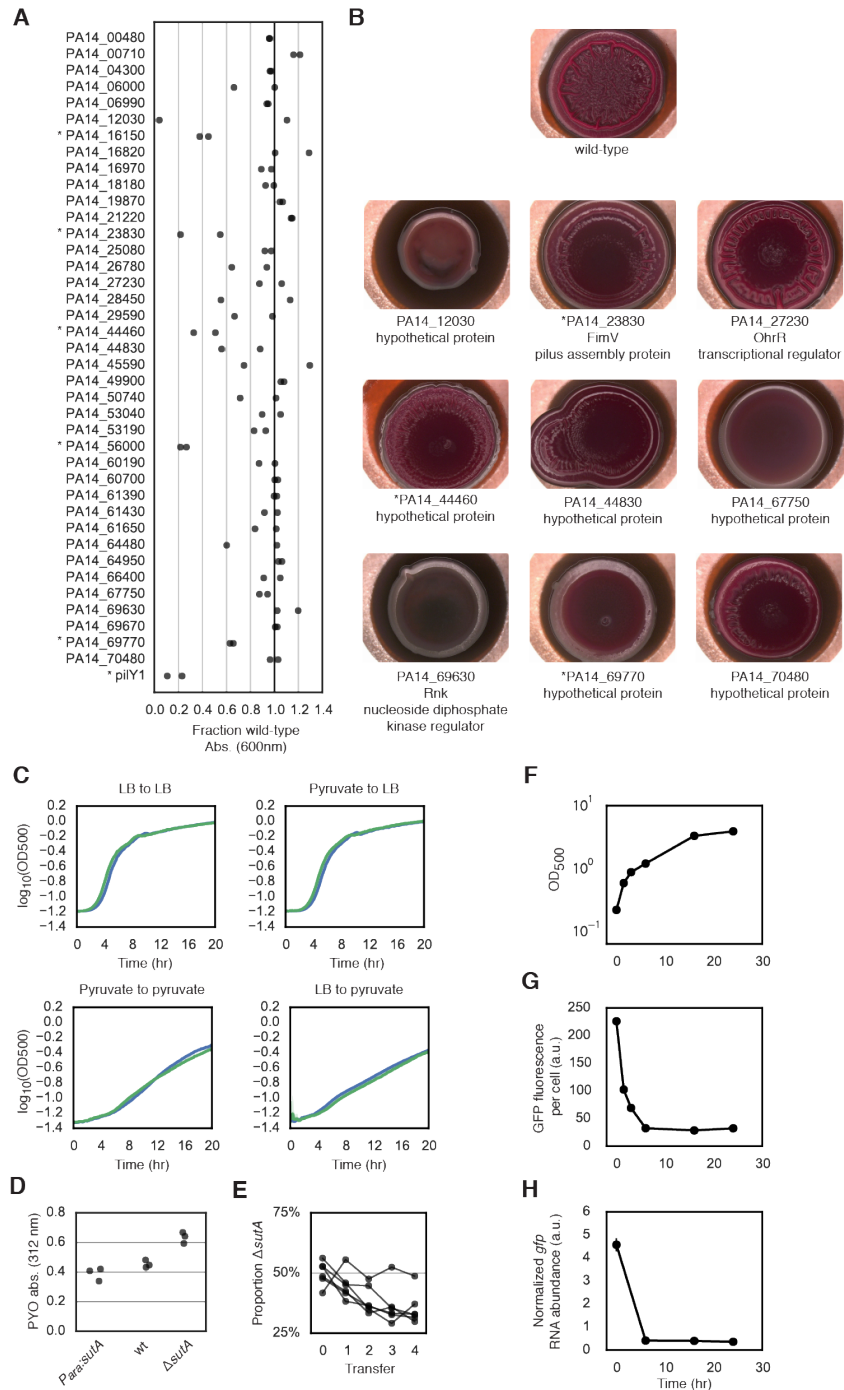


Figure 2.S2: **Phenotype screens and $\Delta sutA$ growth characterization.** (A) Absorbance of Crystal Violet following biofilm growth on polystyrene well plates. Absorbance values were divided by the value for wild type. Each circle indicates the average value for experiments performed on different days, each with three to four biological replicates. Asterisks indicate mutants whose absorbance ratios were significantly less than 1 in both experiments (Student's t-test, $p < 0.05$). The *pilY1* mutant is a control strain known to have a Crystal Violet screen defect. (B) Transposon mutants that exhibited colony biofilm phenotypes different from the wild-type strain. The phenotype screen was performed in duplicate. Representative images are shown. Mutants that were also defective in the Crystal Violet screen are marked with an asterisk. (C) Growth curves for wild-type (green) and $\Delta sutA$ (blue) strains in LB or pyruvate minimal medium. Cultures were grown overnight in the first medium and then diluted into the second medium. For dilution into LB, cultures were diluted to an OD₅₀₀ of 0.001. For dilution into pyruvate, cultures were diluted to an OD₅₀₀ of 0.005. Each line represents the mean of 8 replicates; 95% confidence intervals for the mean are obscured by the thickness of the lines. (D) Absorbance measurements at 312 nm of culture supernatants from wild-type, $\Delta sutA$, and *P_{ara}:sutA* strains. (E) Competition assay results for all six individual replicates. (F-H) A *P_{rpsG}:gfp* cassette was transposed into a neutral locus of the wild-type strain. (F) Optical density, (G) per-cell GFP fluorescence, and (H) *gfp* transcript abundance were measured throughout growth in LB (circles, solid lines). Error bars represent the standard error of biological replicates ($n = 3$), and in some cases are smaller than the marker. RNA abundances were normalized by *oprI*. RNA and GFP measurements are relative to the value for wild type *P_{sutA}:gfp* in LB at time 0 (see Figure 2.3).

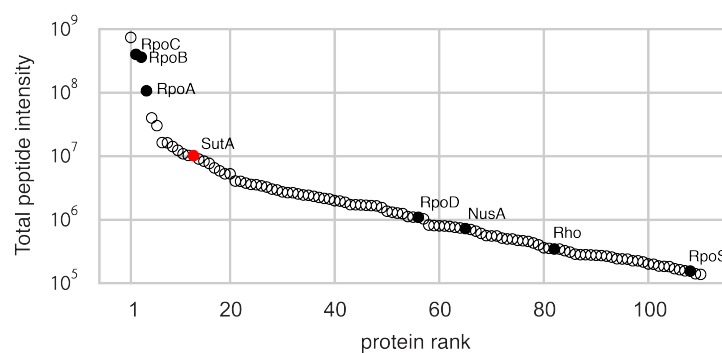


Figure 2.S3: **RpoA co-immunoprecipitated proteins.** Total peptide intensities for proteins that co-precipitated with RpoA. Proteins are ranked by intensity from left to right. The α , β , and β' subunits of RNAP (RpoA, RpoB, and RpoC respectively), as well as the sigma factors RpoD and RpoS, the elongation factor NusA, and the termination factor Rho are shown in black. SutA is shown in red.

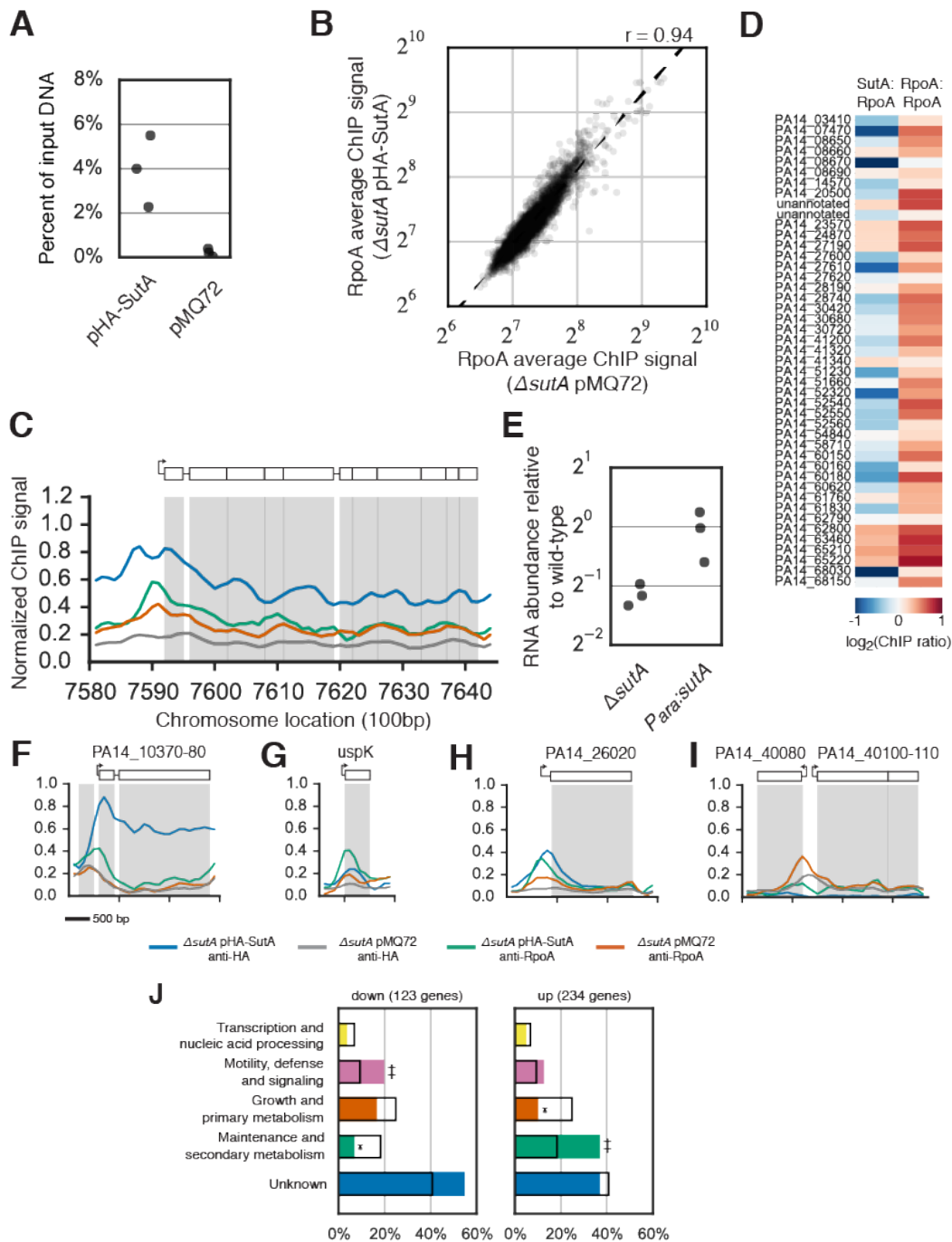


Figure 2.S4: **HA-SutA and RpoA chromatin immunoprecipitation.** (A) DNA yields from chromatin immunoprecipitations against the HA epitope from $\Delta sutA$ pHA-SutA and $\Delta sutA$ pMQ72 relative to input DNA were estimated by quantitative PCR for an intergenic region that was not enriched in the HA-SutA ChIP samples. (B) Average RPKM mapped for all genes from the RpoA immunoprecipitations from $\Delta sutA$ pHA-SutA and $\Delta sutA$ pMQ72 (Pearson's $r = 0.94$). (C) Normalized and scaled ChIP signals for HA immunoprecipitation from $\Delta sutA$ HA-SutA (blue) and $\Delta sutA$ pMQ72 (gray), and for RpoA immunoprecipitation from $\Delta sutA$ pHA-SutA (green) and $\Delta sutA$ pMQ72 (orange) across a chromosomal region containing the S10 (*rpsJ*) ribosomal protein operon. (D) ChIP and RNA-Seq results for tRNA genes. Heatmaps show ratios for HA-SutA ChIP RPKM values compared to RpoA ChIP RPKM values from $\Delta sutA$ pHA-SutA (left column) and RpoA ChIP RPKM values between $\Delta sutA$ pHA-SutA and $\Delta sutA$ pMQ72. tRNAs encoded within rRNA operons are excluded. Because many tRNAs have substantial sequence similarity with each other, only sequencing reads that could be mapped uniquely are displayed, and only tRNAs with at least 10 unique RPKM in the RpoA immunoprecipitation from $\Delta sutA$ pHA-SutA are shown (45 of 62 tRNA genes). (E) qRT-PCR measurements for the 16S leader sequence in the $\Delta sutA$ and *P_{ara}:sutA* strains compared to the wild-type strain. Circles show individual measurements. These data were averaged to generate the expression heatmap shown in Figure 2.5G. (F-I) Normalized ChIP signals at selected genetic loci; scale bar represents 500 bp. Traces are colored as in (C). (J) COG distributions for genes up- and downregulated by SutA, compared to the entire genome. The percentage of genes in each category is indicated with colored bars. Open black bars represent the proportion of the entire genome in each category. Markers indicate categories that are significantly over- (‡) or underrepresented (*) (Fisher's exact test, $p < 0.001$).

References

- (1) Stover, C. K. et al. *Nature* **2000**, *406*, 959–964.
- (2) Potvin, E.; Sanschagrín, F.; Levesque, R. C. *FEMS Microbiol. Rev.* **2008**, *32*, 38–55.
- (3) Salgado, H.; Gama-Castro, S.; Peralta-Gil, M.; Díaz-Peredo, E.; Sánchez-Solano, F.; Santos-Zavaleta, A.; Martínez-Flores, I.; Jiménez-Jacinto, V.; Bonavides-Martínez, C.; Segura-Salazar, J.; Martínez-Antonio, A.; Collado-Vides, J. *Nucleic Acids Res.* **2006**, *34*, D394–D397.
- (4) Raghavan, R.; Groisman, E. A.; Ochman, H. *Genome Res.* **2011**, *21*, 1487–1497.
- (5) Wurtzel, O.; Yoder-Himes, D. R.; Han, K.; Dandekar, A. A.; Edelheit, S.; Greenberg, E. P.; Sorek, R.; Lory, S. *PLoS Pathog.* **2012**, *8*, e1002945.
- (6) Kopf, S. H.; Sessions, A. L.; Cowley, E. S.; Reyes, C.; Sambeek, L. V.; Hu, Y.; Orphan, V. J.; Kato, R.; Newman, D. K. *Proc. Natl. Acad. Sci. U.S.A.* **2016**, *113*, E110–E116.
- (7) Cowley, E. S.; Kopf, S. H.; LaRiviere, A.; Ziebis, W.; Newman, D. K. *mBio* **2015**, *6*, e00767–15.
- (8) Hoboth, C.; Hoffmann, R.; Eichner, A.; Henke, C.; Schmoldt, S.; Imhof, A.; Heesemann, J.; Hogardt, M. *J. Infect Dis.* **2009**, *200*, 118–130.
- (9) Quinn, R. A.; Lim, Y. W.; Maughan, H.; Conrad, D.; Rohwer, F.; Whiteson, K. L. *mBio* **2014**, *5*, e00956–13.
- (10) Glasser, N. R.; Kern, S. E.; Newman, D. K. *Mol. Microbiol.* **2014**, *92*, 399–412.
- (11) Eschbach, M.; Schreiber, K.; Trunk, K.; Buer, J.; Jahn, D.; Schobert, M. *J. Bacteriol.* **2004**, *186*, 4596–4604.
- (12) Wauven, C. V.; Piérard, A.; Kley-Raymann, M.; Haas, D. *J. Bacteriol.* **1984**, *160*, 928–934.
- (13) Alvarez-Ortega, C.; Harwood, C. S. *Mol. Microbiol.* **2007**, *65*, 153–165.
- (14) Trunk, K.; Benkert, B.; Quäck, N.; Münch, R.; Scheer, M.; Garbe, J.; Jänsch, L.; Trost, M.; Wehland, J.; Buer, J.; Jahn, M.; Schobert, M.; Jahn, D. *Environ. Microbiol.* **2010**, *12*, 1719–1733.
- (15) Schreiber, K.; Boes, N.; Eschbach, M.; Jaensch, L.; Wehland, J.; Bjarnsholt, T.; Givskov, M.; Hentzer, M.; Schobert, M. *J. Bacteriol.* **2006**, *188*, 659–668.
- (16) Repoila, F.; Majdalani, N.; Gottesman, S. *Mol. Microbiol.* **2003**, *48*, 855–861.
- (17) Storz, G.; Vogel, J.; Wassarman, K. M. *Mol. Cell* **2011**, *43*, 880–891.

- (18) Dieterich, D. C.; Link, A. J.; Graumann, J.; Tirrell, D. A.; Schuman, E. M. *Proc. Natl. Acad. Sci. U.S.A.* **2006**, *103*, 9482–9487.
- (19) Dieterich, D. C.; Lee, J. J.; Link, A. J.; Graumann, J.; Tirrell, D. A.; Schuman, E. M. *Nat. Protoc.* **2007**, *2*, 532–540.
- (20) Liberati, N. T.; Urbach, J. M.; Miyata, S.; Lee, D. G.; Drenkard, E.; Wu, G.; Villanueva, J.; Wei, T.; Ausubel, F. M. *Proc. Natl. Acad. Sci. U.S.A.* **2006**, *103*, 2833–2838.
- (21) Stewart, P. S.; Franklin, M. J. *Nat. Rev. Microbiol.* **2008**, *6*, 199–210.
- (22) Michel, G. P. F.; Aguzzi, A.; Ball, G.; Soscia, C.; Bleves, S.; Voulhoux, R. *Microbiology* **2011**, *157*, 1945–1954.
- (23) Lau, G. W.; Hassett, D. J.; Ran, H.; Kong, F. *Trends Microbiol.* **2004**, *10*, 599–606.
- (24) Wang, Y.; Kern, S. E.; Newman, D. K. *J. Bacteriol.* **2010**, *192*, 365–369.
- (25) Dietrich, L. E. P.; Price-Whelan, A.; Petersen, A.; Whiteley, M.; Newman, D. K. *Mol. Microbiol.* **2006**, *61*, 1308–1321.
- (26) Fröhlich, K. S.; Vogel, J. *Curr. Opin. Microbiol.* **2009**, *12*, 674–682.
- (27) Mooney, R. A.; Davis, S. E.; Peters, J. M.; Rowland, J. L.; Ansari, A. Z.; Landick, R. *Mol. Cell* **2009**, *33*, 97–108.
- (28) Kusuya, Y.; Kurokawa, K.; Ishikawa, S.; Ogasawara, N.; Oshima, T. *J. Bacteriol.* **2011**, *193*, 3090–3099.
- (29) Zhang, Y.; Mooney, R. A.; Grass, J. A.; Sivaramakrishnan, P.; Herman, C.; Landick, R.; Wang, J. D. *Mol. Cell* **2014**, *53*, 766–778.
- (30) Dennis, P. P.; Ehrenberg, M.; Bremer, H. *Microbiol. Mol. Biol. Rev.* **2004**, *68*, 639–668.
- (31) Michiels, J.; Dirix, G.; Vanderleyden, J.; Xi, C. *Trends Microbiol.* **2001**, *9*, 164–168.
- (32) Kang, Y.; Lunin, V. V.; Skarina, T.; Savchenko, A.; Schurr, M. J.; Hoang, T. T. *Mol. Microbiol.* **2009**, *73*, 120–136.
- (33) Tatusov, R. L. et al. *BMC Bioinformatics* **2003**, *4*, 41.
- (34) Paul, B. J.; Barker, M. M.; Ross, W.; Schneider, D. A.; Webb, C.; Foster, J. W.; Gourse, R. L. *Cell* **2004**, *118*, 311–322.
- (35) Perederina, A.; Svetlov, V.; Vassilyeva, M. N.; Tahirov, T. H.; Yokoyama, S.; Artsimovitch, I.; Vassilyev, D. G. *Cell* **2004**, *118*, 297–309.
- (36) Perron, K.; Comte, R.; Van Delden, C. *Mol. Microbiol.* **2005**, *56*, 1087–1102.
- (37) Lemke, J. J.; Sanchez-Vazquez, P.; Burgos, H. L.; Hedberg, G.; Ross, W.; Gourse, R. L. *Proc. Natl. Acad. Sci. U.S.A.* **2011**, *108*, 5712–5717.

- (38) Blaby-Haas, C. E.; Furman, R.; Rodionov, D. A.; Artsimovitch, I.; de Crécy-Lagard, V. *Mol. Microbiol.* **2011**, *79*, 700–715.
- (39) López-Sánchez, A.; Jiménez-Fernández, A.; Calero, P.; Gallego, L. D.; Govantes, F. *Environ. Microbiol. Rep.* **2013**, *5*, 679–685.
- (40) Tehranchi, A. K.; Blankschien, M. D.; Zhang, Y.; Halliday, J. A.; Srivatsan, A.; Peng, J.; Herman, C.; Wang, J. D. *Cell* **2010**, *141*, 595–605.
- (41) Gummesson, B.; Lovmar, M.; Nyström, T. *J. Biol. Chem.* **2013**, *288*, 21055–21064.
- (42) Withers, R.; Doherty, G. P.; Jordan, M.; Yang, X.; Dixon, N. E.; Lewis, P. J. *Mol. Microbiol.* **2014**, *93*, 1130–1143.
- (43) Dietrich, L. E. P.; Okegbe, C.; Price-Whelan, A.; Sakhtah, H.; Hunter, R. C.; Newman, D. K. *J. Bacteriol.* **2013**, *195*, 1371–1380.
- (44) Müsken, M.; Di Fiore, S.; Dötsch, A.; Fischer, R.; Häussler, S. *Microbiology* **2010**, *156*, 431–441.
- (45) Mahdavi, A.; Szychowski, J.; Ngo, J. T.; Sweredoski, M. J.; Graham, R. L. J.; Hess, S.; Schneewind, O.; Mazmanian, S. K.; Tirrell, D. A. *Proc. Natl. Acad. Sci. U.S.A.* **2014**, *111*, 433–438.
- (46) Boersema, P. J.; Rajmakers, R.; Lemeer, S.; Mohammed, S.; Heck, A. J. R. *Nat. Protoc.* **2009**, *4*, 484–494.
- (47) Gilbert, K. B.; Kim, T. H.; Gupta, R.; Greenberg, E. P.; Schuster, M. *Mol. Microbiol.* **2009**, *73*, 1072–1085.